

# Theoretical Investigation of the Instantaneous Folding Force during the First Fold Creation in a Square Column

A. Niknejad, G. H. Liaghat, A. H. Behraves, and H. Moslemi Naeini

**Abstract**—In this paper, a theoretical formula is presented to predict the instantaneous folding force of the first fold creation in a square column under axial loading. Calculations are based on analysis of “Basic Folding Mechanism” introduced by Wierzbicki and Abramowicz. For this purpose, the sum of dissipated energy rate under bending around horizontal and inclined hinge lines and dissipated energy rate under extensional deformations are equated to the work rate of the external force on the structure. Final formula obtained in this research, reasonably predicts the instantaneous folding force of the first fold creation versus folding distance and folding angle and also predicts the instantaneous folding force instead of the average value. Finally, according to the calculated theoretical relation, instantaneous folding force of the first fold creation in a square column was sketched versus folding distance and was compared to the experimental results which showed a good correlation.

**Keywords**—Instantaneous force, Folding force, Honeycomb, Square column.

## I. INTRODUCTION

HONEYCOMB is categorized as a thin-walled structure, and due to its special advantages such as high energy absorption is widely used in various industries. Also sandwich panel with honeycomb core is also used in transportation industry and aerospace systems, because of its high strength and stiffness to the weight ratio. Among honeycomb properties, its folding behavior under axial loading is the most important, since the highest portion of the absorbed energy occurs during this mechanism.

In recent decades, many researchers have investigated the honeycomb behavior under the various loading. Average folding force of a “Basic Folding Mechanism” is calculated by Wierzbicki and Abramowicz [1]. Wierzbicki and Heyduk investigated the extensional folding modes in an angular element [2]. Abramowicz calculated the effective folding distance in thin-walled columns [3]. Then dynamics folding of a square column was experimentally analyzed by Abramowicz

and Jones [4]. Wierzbicki and Abramowicz carried out an experimental and theoretical investigation on the crushing process in polyurethane foam-filled square columns [5]. Then they theoretically calculated the mean folding force in square and hexagonal columns by introducing Corner Element with selectable angle [6]. Liaghat *et al.* compared the theoretical results with those of experimental [7] and checked analytical relations and then theoretically and numerically investigated honeycomb behavior under impact [8]–[13]. Effect of metal fillers such as Aluminum foam in a square column and the behavior of the column under bending were studied by Santosa and Wierzbicki through experimental and numerical methods [14, 15]. Chen *et al.* analytically calculated the mean folding force in a multi-cell square column [16]. Zhang *et al.* calculated the mean crushing force in multi-cell columns, based on Superfolding Element [17].

Through reviewing of the published works on folding behavior of the columns and honeycombs, reveals that mean folding force in uni-cell and multi-cell columns is basically calculated theoretically. In this paper, the instantaneous folding force of the first fold creation in a “Basic Folding Mechanism” is calculated analytically. The instantaneous folding force of the first fold creation in a square column is then calculated.

On the other hand, in this paper, the instantaneous folding force of the first fold creation is calculated instead of an average value for folding force in a square column, as a small model of multi-cell honeycombs, analytically.

## II. THEORY

### A. Theoretical Calculation by Wierzbicki

These theoretical calculations are based on Wierzbicki and Abramowicz’s research on Work and Energy concept. For this purpose, a “Basic Folding Mechanism” was introduced and the dissipated energy rate by this mechanism was calculated [1].

A. Niknejad is with the Mechanical Engineering Department, Tarbiat Modares University, Tehran, Iran (phone: 021-8288-3387; fax: 0351--726--2882; e-mail: niknejad@pnu.ac.ir).

G. H. Liaghat is with the Mechanical Engineering Department, Tarbiat Modares University, Tehran, Iran (e-mail: ghli530@modares.ac.ir).

A. H. Behraves is with the Mechanical Engineering Department, Tarbiat Modares University, Tehran, Iran (e-mail: amirhb@modares.ac.ir).

H. Moslemi N. is with the Mechanical Engineering Department, Tarbiat Modares University, Tehran, Iran (e-mail: moslemi@modares.ac.ir).

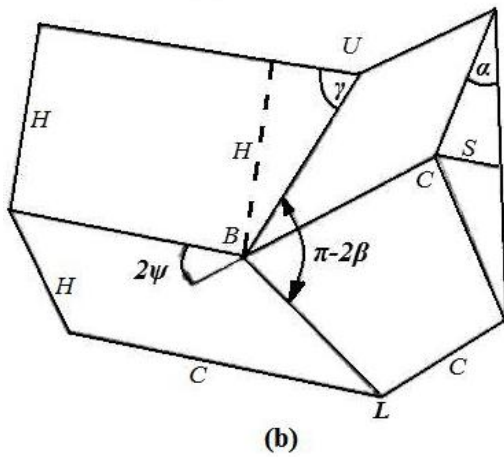
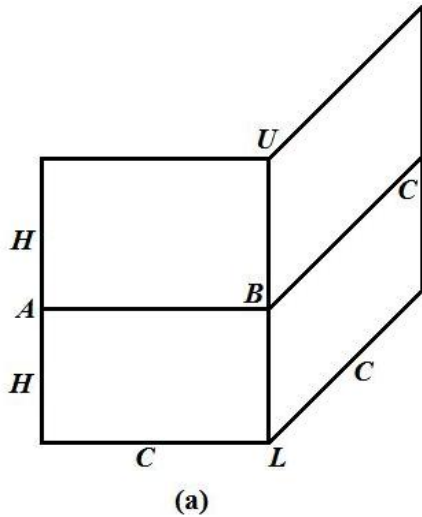


Fig. 1 Basic Folding Mechanism, (a) before folding, (b) after folding [1]

### B. Basic Folding Mechanism

Wierzbicki and Abramowicz introduced Basic Folding Mechanism according to the Fig. 1. At the start time  $\alpha = 0$ , and  $\gamma = 90^\circ$ . At commence of folding,  $\alpha$  increases and  $\gamma$  decreases, continuously. When folding is initiated,  $\gamma$  and  $\beta$  vary versus  $\alpha$  and  $\psi_0$  according to the followings [1]:

$$\operatorname{tg} \gamma = \frac{\operatorname{tg} \psi_0}{\operatorname{Sin} \alpha}, \quad \operatorname{tg} \beta = \frac{\operatorname{tg} \gamma}{\operatorname{Sin} \psi_0} \quad (1)$$

Instantaneous folding distance designated by  $\delta$ , indicates the decreasing axial distance between upper and lower edges of Basic Folding Mechanism. This quantity as shown in Fig. 2 is calculated as following:

$$\delta = 2H \cdot (1 - \operatorname{Cos} \alpha) \quad (2)$$

where the initial height of the Basic Folding Mechanism is

defined by  $2H$ . Differentiating the above relation yields:

$$\dot{\delta} = 2H \cdot \operatorname{Sin} \alpha \cdot \dot{\alpha} \quad (3)$$

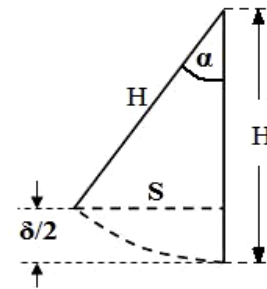


Fig. 2 Half of the folding wavelength

### C. Dissipated Energy Rate

In folding process, the dissipated energy rate is resulted from the continuous and discontinuous velocity fields as shown in following [1]:

$$\dot{E}_{\text{int}} = \int_S (M^{\alpha\beta} \dot{\kappa}_{\alpha\beta} + N^{\alpha\beta} \dot{\lambda}_{\alpha\beta}) \cdot dS + \int_L M_0 \dot{\theta} \cdot d\ell \quad (4)$$

which  $N^{\alpha\beta}$ ,  $M^{\alpha\beta}$ ,  $\dot{\kappa}_{\alpha\beta}$ , and  $\dot{\lambda}_{\alpha\beta}$  are stress resultants, stress couples, the rate of curvature, and the rate of extension, in the continuous deformation field, respectively [1]. Note that both the extent of continuous plastic deformations  $S$  and the length of hinge lines  $\ell$  increase during the deformation progresses.  $\theta$  is a finite rotation around every hinge line. In above formula, the first integral calculates the dissipated energy of extensional deformation on the small area that is called toroidal surface and the second integral calculates the dissipated energy of the inextensional deformation, or in other word, dissipated energy of bending around hinge lines.

Performing first integration results in [1]:

$$\dot{E}_1 = \frac{4N_0 b H \pi}{(\pi - 2\psi_0) \cdot \operatorname{tg} \psi_0} \cdot \operatorname{Cos} \alpha \cdot \left\{ \operatorname{Sin} \psi_0 \cdot \operatorname{Sin} \left( \frac{\pi - 2\psi_0}{\pi} \cdot \beta \right) + \operatorname{Cos} \psi_0 \left[ 1 - \operatorname{Cos} \left( \frac{\pi - 2\psi_0}{\pi} \cdot \beta \right) \right] \right\} \cdot \dot{\alpha} \quad (5)$$

Where  $b$  is the small radius of toroidal surface [1] and angles  $\alpha$ ,  $\beta$ , and  $\psi_0$  are shown in Fig. 1. The dissipated energy rate in the above equation refers to the dissipated energy rate of the extensional deformation on toroidal surface, that is the value of the first integral in (4).

The second integral in (4) was separately calculated for fixed horizontal hinge lines and then for inclined hinge lines. In other word, the second integral in this equation that shows inextensional deformations, involves bending around fixed horizontal hinge lines AB, BC and bending around inclined hinge lines UB, BL designated by  $\dot{E}_2$ ,  $\dot{E}_3$ , respectively.

Dissipated energy rate of bending around fixed horizontal

hinge lines AB, BC, designated by  $\dot{E}_2$ , is equated to [1]:

$$\dot{E}_2 = 2M_0 C \dot{\theta} = 2M_0 C \dot{\alpha} \quad (6)$$

where C is the width of every edge of the Basic Folding Mechanism. The dissipated energy rate of bending around inclined hinge lines UB, BL is equal to [1]:

$$\dot{E}_3 = 2M_0 L \dot{\theta} = 4M_0 \cdot \frac{H^2}{b} \cdot \frac{1}{\text{tg} \psi_0} \cdot \frac{\text{Cos} \alpha}{\text{Sin} \gamma} \cdot \dot{\alpha} \quad (7)$$

#### D. Instantaneous Folding Force Calculation in BFM

First, the instantaneous folding force is calculated. Thus, the summation of the internal dissipated energy rate in a Basic Folding Mechanism, which is calculated as (4), is written as following:

$$\dot{E}_{\text{int}} = \dot{E}_1 + \dot{E}_2 + \dot{E}_3 \quad (8)$$

where  $\dot{E}_1$ ,  $\dot{E}_2$  and  $\dot{E}_3$  are resulted of (5), (6) and (7) respectively.

The external work rate in a compressing process of Basic Folding Mechanism is calculated as below:

$$\dot{E}_{\text{ext}} = P \cdot \dot{\delta} = P \cdot 2H \cdot \text{Sin} \alpha \cdot \dot{\alpha} \quad (9)$$

where P is the external force on the Basic Folding Mechanism under the axial loading. Thus, using the following equation:

$$\dot{E}_{\text{ext}} = \dot{E}_{\text{int}} \quad (10)$$

which shows the external work rate, required for compressing in a Basic Folding Mechanism mode is equated with the internal dissipated energy rate, and the following relation is reached:

$$P \cdot 2H \cdot \text{Sin} \alpha \cdot \dot{\alpha} = \dot{E}_1 + \dot{E}_2 + \dot{E}_3 \quad (11)$$

Substituting (5), (6) and (7) in (11) and dividing both sides of the relation by  $2H\dot{\alpha}\text{Sin} \alpha$ , results in:

$$P = 2M_0 \cdot \frac{H}{b} \cdot \frac{\text{Cotg} \alpha}{\text{tg} \psi_0} \cdot \frac{1}{\text{Sin} \gamma} + \frac{M_0}{\text{Sin} \alpha} \cdot \frac{C}{H} + \frac{2N_0 b \pi}{(\pi - 2\psi_0)} \cdot \frac{\text{Cotg} \alpha}{\text{tg} \psi_0} \cdot \left\{ \text{Sin} \psi_0 \cdot \text{Sin} \left( \frac{\pi - 2\psi_0}{\pi} \cdot \beta \right) + \text{Cos} \psi_0 \left[ 1 - \text{Cos} \left( \frac{\pi - 2\psi_0}{\pi} \cdot \beta \right) \right] \right\} \quad (12)$$

According to [1] following relation is obtained:

$$M_0 = \frac{\sigma_0 h^2}{4} = \sigma_0 h \cdot \left( \frac{h}{4} \right) = N_0 \left( \frac{h}{4} \right) \Rightarrow N_0 = \frac{4M_0}{h} \quad (13)$$

where the thickness of the Basic Folding Mechanism is defined by h. Hence:

$$P = 2M_0 \cdot \frac{H}{b} \cdot \frac{\text{Cotg} \alpha}{\text{tg} \psi_0} \cdot \frac{1}{\text{Sin} \gamma} + \frac{M_0}{\text{Sin} \alpha} \cdot \frac{C}{H} + \frac{8M_0 b \pi}{(\pi - 2\psi_0) h} \cdot \frac{\text{Cotg} \alpha}{\text{tg} \psi_0} \cdot \left\{ \text{Sin} \psi_0 \cdot \text{Sin} \left( \frac{\pi - 2\psi_0}{\pi} \cdot \beta \right) + \text{Cos} \psi_0 \left[ 1 - \text{Cos} \left( \frac{\pi - 2\psi_0}{\pi} \cdot \beta \right) \right] \right\} \quad (14)$$

Equation (14) is rewritten as:

$$\frac{P}{M_0} = A_1 \frac{b}{h} + A_2 \frac{C}{H} + A_3 \frac{H}{b} \quad (15)$$

$$A_1 = \frac{8\pi}{(\pi - 2\psi_0)} \cdot \frac{\text{Cotg} \alpha}{\text{tg} \psi_0} \cdot \left\{ \text{Sin} \psi_0 \cdot \text{Sin} \left( \frac{\pi - 2\psi_0}{\pi} \cdot \beta \right) + \text{Cos} \psi_0 \left[ 1 - \text{Cos} \left( \frac{\pi - 2\psi_0}{\pi} \cdot \beta \right) \right] \right\}$$

$$A_2 = \frac{1}{\text{Sin} \alpha}$$

$$A_3 = \frac{\text{Cotg} \alpha}{\text{tg} \psi_0} \cdot \frac{2}{\text{Sin} \gamma}$$

This relation is similar to Wierzbicki and Abramowicz's relation [1], for predicting the average value of the folding force, where these corresponding equations just differed by values of  $A_1$ ,  $A_2$  and  $A_3$ . Naturally, the folding process led to the least possible amount of the instantaneous folding force. So the following limitations should be considered:

$$\frac{\partial P}{\partial H} = 0, \quad \frac{\partial P}{\partial b} = 0 \quad (16)$$

Equation (16) results in two equations and two unknown parameters. Hence H and b are calculated to show half of the folding wavelength and small radius of the toroidal surface, respectively:

$$b = \sqrt[3]{A_2 A_3 / A_1^2} \cdot \sqrt[3]{C h^2} \quad (17)$$

$$H = \sqrt[3]{A_2^2 / A_1 A_3} \cdot \sqrt[3]{C^2 h}$$

By substituting (17) into (15), following relation is obtained:

$$\frac{P}{M_0} = 3 \sqrt[3]{A_1 A_2 A_3} \cdot \sqrt[3]{C/h} \quad (18)$$

#### E. Instantaneous Folding Force in Square Column

A column with a square cross section is a small model of the square cell honeycomb. This column can be produced by joining four Basic Folding Mechanisms, illustrated in Fig. 1. In this situation, the length of each edge of the square is equal to 2C.

For a square column, the second side of (11) must be fourfolded, namely:

$$P \cdot 2H \cdot \sin \alpha \cdot \dot{\alpha} = 4\dot{E}_1 + 4\dot{E}_2 + 4\dot{E}_3 \quad (19)$$

The term  $\dot{E}_2$  from (6) refers to bending around the horizontal hinge lines, while horizontal edges are simple supported. In reality, these edges are clamped and so  $\dot{E}_2$  should be doubled. Thus, (19) is rewritten as following:

$$P \cdot 2H \cdot \sin \alpha \cdot \dot{\alpha} = 4\dot{E}_1 + 8\dot{E}_2 + 4\dot{E}_3 \quad (20)$$

Noting the square column geometry, we find that the external angle of the square column is  $2\psi_0 = 90^\circ$  and so  $\psi_0 = 45^\circ$ . By substituting values of  $\dot{E}_1$ ,  $\dot{E}_2$  and  $\dot{E}_3$  from (5), (6) and (7) into (20) and recalculating, the results predict the instantaneous folding force of a square column:

$$\frac{P}{M_0} = A_1 \frac{b}{h} + A_2 \frac{C}{H} + A_3 \frac{H}{b}$$

$$A_1 = 32\sqrt{2} \cdot \text{Cotg} \alpha \cdot \left[ \sin\left(\frac{\beta}{2}\right) - \cos\left(\frac{\beta}{2}\right) + 1 \right] \quad (21)$$

$$A_2 = \frac{8}{\sin \alpha}$$

$$A_3 = \frac{8 \text{Cotg} \alpha}{\sin \gamma}$$

Now, by applying minimum conditions from (16) to the square column relations, a formula similar to (18) is obtained, with only difference in values of  $A_1$ ,  $A_2$  and  $A_3$ , which are coefficients of (21).

Multiplying these coefficients, results in:

$$A_1 A_2 A_3 = \frac{2048 \sqrt{2} \cdot \text{Cotg}^2 \alpha}{\sin \alpha \cdot \sin \gamma} \cdot \left[ \sin\left(\frac{\beta}{2}\right) - \cos\left(\frac{\beta}{2}\right) + 1 \right] \quad (22)$$

Considering the purpose, which is calculating of the instantaneous folding force versus value of angle  $\alpha$  or axial displacement  $\delta$  in each time, the trigonometry function of angles  $\gamma$  and  $\beta$  in (22) should be calculated as a function of angle  $\alpha$ .

In (1) and by noting that  $\psi_0 = 45^\circ$  for square columns, following relation is obtained between  $\gamma$  and  $\alpha$ :

$$\frac{1}{\sin \gamma} = \sqrt{1 + \sin^2 \alpha} \quad (23)$$

Also from (1) and the trigonometry union, following relations are resulted between  $\beta$  and  $\alpha$ :

$$\sin\left(\frac{\beta}{2}\right) = \sqrt{\frac{\sqrt{2 + \sin^2 \alpha} - \sin \alpha}{2\sqrt{2 + \sin^2 \alpha}}} \quad (24)$$

and,

$$\cos\left(\frac{\beta}{2}\right) = \sqrt{\frac{\sqrt{2 + \sin^2 \alpha} + \sin \alpha}{2\sqrt{2 + \sin^2 \alpha}}} \quad (25)$$

Hence, by substituting (23), (24) and (25) in (22), the final relation for the instantaneous folding force is obtained:

$$\frac{P}{M_0} = 3\sqrt[3]{A_1 A_2 A_3} \cdot \sqrt[3]{C/h} \quad (26)$$

$$A_1 A_2 A_3 = \frac{2048 \sqrt{2} \cdot \text{Cotg}^2 \alpha \cdot \sqrt{1 + \sin^2 \alpha}}{\sin \alpha} \cdot \left[ \sqrt{\frac{\sqrt{2 + \sin^2 \alpha} - \sin \alpha}{2\sqrt{2 + \sin^2 \alpha}}} - \sqrt{\frac{\sqrt{2 + \sin^2 \alpha} + \sin \alpha}{2\sqrt{2 + \sin^2 \alpha}}} + 1 \right]$$

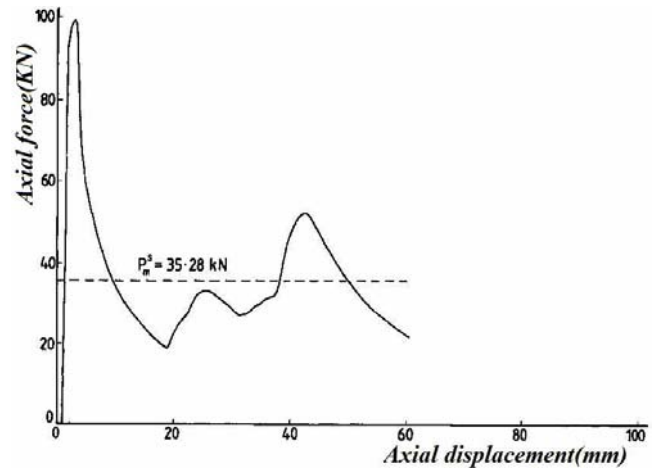


Fig. 3 Experimental diagram of the folding force versus the axial displacement [4]

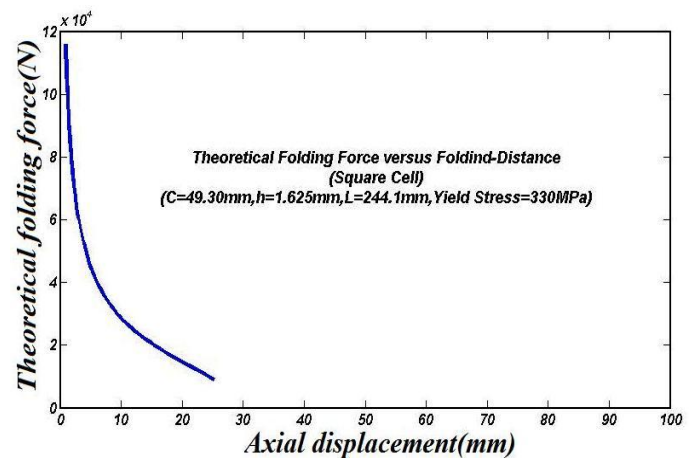


Fig. 4 Theoretical diagram of the folding force versus the folding distance during the first fold creation

### III. RESULTS AND DISCUSSION

The predicted results of the instantaneous folding force by (26) were investigated. The experimental diagram, Fig. 3 shows the instantaneous folding force versus the folding distance in a square steel column with the length  $L = 244.1mm$ , the wall thickness  $h = 1.625mm$ , and half of the edge  $C = 49.30mm$  [4]. As this diagram shows and considering the physical behavior, when starting every fold, the folding force increased from a minimum value and then follows decreasing way and with each completed folding, reaches a relative minimum value. Then by starting the next fold, follows increasing and decreasing cycle, again. To compare, as a result of (26), the instantaneous folding force in this column with  $L = 244.1mm$ ,  $h = 1.625mm$  and  $C = 49.30mm$  versus the folding distance is shown in Fig. 4. Comparing Fig. 3 and Fig. 4 shows that a presented theoretical relation in this paper can predict the first peak in real folding force of the first fold creation versus the folding distance with a good accuracy. To better comparing, diagrams of Fig. 3 and Fig. 4 are drawn in the same diagram as shown in Fig. 5. As shown, values of the first peak in experimental folding force-folding distance curves are in a good agreement with results of (26). Also this theoretical relation predicts the folding force variations of the first fold versus the folding distance with a good correlation. This result was obtained by comparing the two diagram slopes in different zones.

Sometimes, the predicted value of the theoretical (26) is smaller than the experimental value. This is affected of calculations of (26), where just three mechanisms of dissipated energy are assumed. These mechanisms are one extensional deformation mode and two bending deformation modes. Although the experimental and theoretical results are different, this small difference between two answers is logical and eligible.

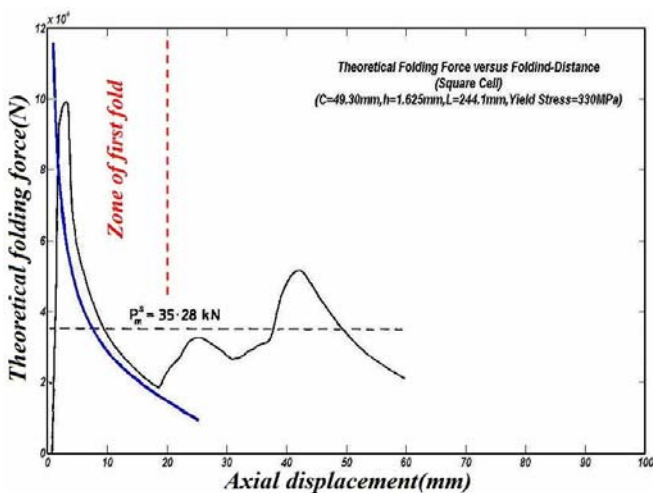


Fig. 5 Theoretical and experimental diagram of the folding force versus the folding distance

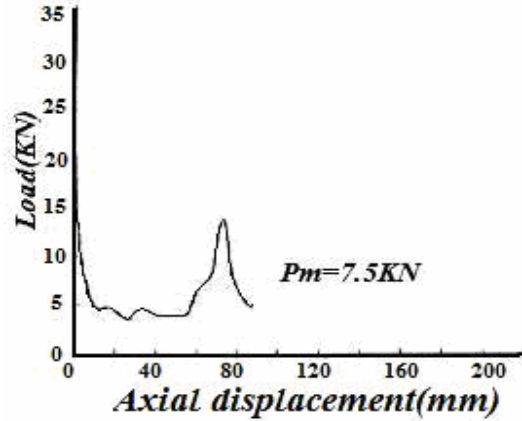


Fig. 6 Experimental diagram of the folding force versus the folding distance [18]

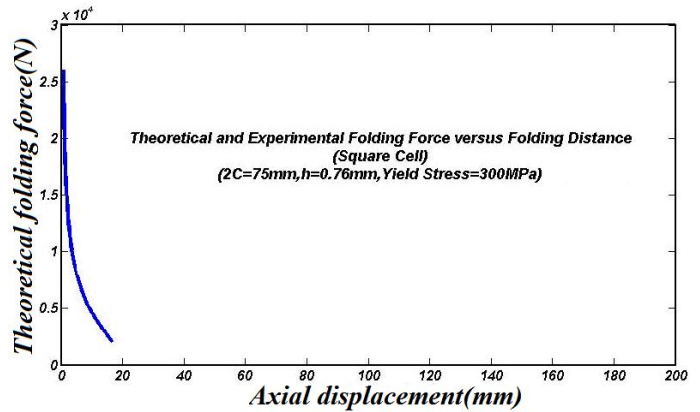


Fig. 7 Theoretical diagram of the folding force versus the folding distance

The instantaneous folding force diagram of a square column with the edge length  $2C = 75mm$  and wall thickness  $h = 0.76mm$  that prepared by Reid *et al.* [18] is shown in Fig. 6. Also the instantaneous folding force diagram of this column with above dimensions is drawn in Fig. 7. Comparing Fig. 6 and Fig. 7 results that the calculated theoretical relation in this paper can predict the maximum value of crushing force in a square column with a good accuracy and this relation can predict the instantaneous folding force variations in a square column during the first fold creation and predict the axial displacement variations of this column with a very good accuracy.

For better comparing, both diagrams, Fig. 6 and Fig. 7 are drawn together in Fig. 8. As shown, two diagrams have good correlation with each other, which again shows the correlation of the theoretical relation in this paper to the test results.

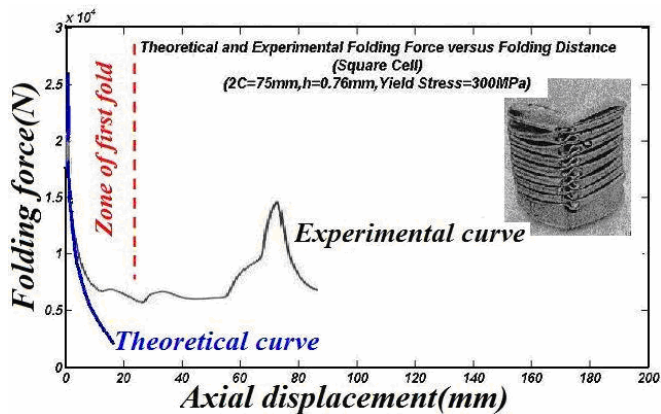


Fig. 8 Theoretical and experimental diagram of the folding force versus the folding distance

#### IV. CONCLUSION

In this paper, a theoretical relation is presented to predict the instantaneous folding force and its variations versus the axial displacement of a column. By using these relations, the instantaneous folding force of the first fold creation was obtained versus the axial displacement of the column with a acceptable accuracy.

Results of the theoretical predictions of this equation were compared with the experimental results of other researchers on the square column and a good correlation was obtained.

#### REFERENCES

- [1] T. Wierzbicki, W. Abramowicz, "On the Crushing Mechanics of Thin-Walled Structures", *Journal of Applied Mechanics*; Vol. 50, pp. 727-734, 1983.
- [2] R. J. Hayduk, and T. Wierzbicki, "Extensional Collapse Modes of Structural Members", *Computers and Structures*, vol. 18, pp. 447-458, 1984.
- [3] W. Abramowicz, "The Effective Crushing Distance in Axially Compressed Thin-Walled Metal Columns", *International Journal of Impact Engineering*, vol.1, No.3, pp. 309-317, 1983.
- [4] W. Abramowicz, and N. Jones, "Dynamic Axial Crushing of Square Tubes", *International Journal of Impact Engineering*, vol. 2, No. 2, pp. 179-208, 1984.
- [5] W. Abramowicz, and T. Wierzbicki, "Axial Crushing of Foam-Filled Columns", *International Journal of Mechanical Sciences*, vol. 30, No. 3/4, pp. 263-271, 1988.
- [6] W. Abramowicz, and T. Wierzbicki, "Axial Crushing of Multi-corner Sheet Metal Columns", *Journal of Applied Mechanics*, vol. 56, pp. 113-120, 1989.
- [7] G. H. Liaghat, and A. Alavinia, "A Comment on the Axial Crush of Metallic Honeycombs by Wu and Jiang", *International Journal of Impact Engineering*, vol. 28, pp. 1143-1146, 2003.
- [8] G. H. Liaghat, H. R. Daghighi, M. Sedighi, and A. Alavinia, "Dynamic Crushing of Honeycomb panel under Impact of Cylindrical Projectile (Persian)", *Amirkabir Journal*, vol.53, pp. 68-79, 2002.
- [9] G. H. Liaghat, M. Sedighi, H. R. Daghighi, and A. Alavinia, "Crushing of Metal honeycomb structures under Quasi-static Loads (Persian)", *Tehran University Journal*, vol. 37, No. 1, pp. 145-156, 2003.
- [10] J. Zamani, M. Soleimani, A. Darvizeh, and G. H. Liaghat, "Numerical Analysis of Full Folding of Thin-Walled Structures with Square Cross-section by LS-DYNA", *Fourteenth International Conference of Mechanical Engineering*, Iran, 2006.
- [11] A. Alavinia, and G. H. Liaghat, "Investigation of Properties and Quasi-static Analysis of Honeycombs", *Twelfth International Conference of Mechanical Engineering*, Tehran, Iran, 2004.

- [12] A. Alavinia, and G. H. Liaghat, "Dynamic Crushing of Thin-Walled Columns under Impact of Projectile", *Twelfth International Conference of Mechanical Engineering*, Tehran, Iran, 2004.
- [13] J. Zamani, and G. H. Liaghat, "Effect of Honeycomb Main Properties under Impact Loads", *Tenth International Conference of Mechanical Engineering*, Iran, 2002, pp. 687-689.
- [14] S. Santosa, and T. Wierzbicki, "Effect of Ultra light Metal Filler on the Bending Collapse Behavior of Thin-Walled Prismatic Columns", *International Journal of Mechanical Sciences*, vol. 41, pp. 995-1019, 1999.
- [15] S. Santosa, T. Wierzbicki, A. G. Hanssen, and M. Langseth, "Experimental and Numerical Studies of Foam-Filled Sections", *International Journal of Impact Engineering*, vol. 24, pp. 509-534, 2000.
- [16] W. Chen, and T. Wierzbicki, "Relative Merits of Single-Cell, Multi-Cell and Foam-Filled Thin-Walled Structures in Energy Absorption", *Thin-Walled Structures*, vol. 39, pp. 287-306, 2001.
- [17] Xiong Zhang, G. Cheng, and Hui Zhang, "Theoretical Prediction and Numerical Simulation of Multi-Cell Square Thin-Walled Structures", *Thin-Walled Structures*, vol. 44, pp. 1185-1191, 2006.
- [18] S. R. Reid, T. Y. Reddy, and M. D. Gray, "Static and Dynamic Axial Crushing of Foam-Filled Sheet Metal Tubes", *International Journal of Mechanical Sciences*, vol. 28, No.5, pp. 295-322, 1986.